Structure and Function of the N-terminal Nucleolin Binding Domain of Nuclear Valosin-containing Protein-like 2 (NVL2) Harboring a Nucleolar Localization Signal*[S]

Yoshie Fujiwara[‡§¶], Ken-ichiro Fujiwara[‖**], Natsuko Goda[‡¶], Naoko Iwaya[‡¶‡‡], Takeshi Tenno[‡§], Masahiro Shirakawa[‡‡], and Hidekazu Hiroaki[‡§¶1]

From the ‡Division of Structural Biology, Graduate School of Medicine, and the §Global Center of Excellence Program for Integrative Membrane Biology, Kobe University, 7-5-1 Kusunokicho, Chuo-ku, Kobe, Hyogo 650-0017, Japan, the ¶Institute for Bioinformatics Research and Development, Japan Science and Technology Agency, Kawaguchi Center Building, 4-1-8, Honcho, Kawaguchi, Saitama 332-0012, Japan, the ‖Field of Supramolecular Biology, International Graduate School of Arts and Sciences, Yokohama City University, 1-7-29 Suehirocho, Tsurumi-ku, Yokohama, Kanagawa 230-0045, Japan, **Shionogi Research Laboratories, Shionogi & Co., Ltd., 5-12-4 Sagisu, Fukushima-ku, Osaka 553-0002, Japan, and the ‡‡Department of Molecular Engineering, Graduate School of Engineering, Kyoto University, Kyoto-daigaku Katsura, Nishikyo-ku, Kyoto 615-8510, Japan

The N-terminal regions of AAA-ATPases (ATPase associated with various cellular activities) often contain a domain that defines the distinct functions of the enzymes, such as substrate specificity and subcellular localization. As described herein, we have determined the solution structure of an N-terminal unique domain isolated from nuclear valosin-containing protein (VCP)-like protein 2 (NVL2^{UD}). NVL2^{UD} contains three α helices with an organization resembling that of a winged helix motif, whereas a pair of β-strands is missing. The structure is unique and distinct from those of other known type II AAA-ATPases, such as VCP. Consequently, we identified nucleolin from a HeLa cell extract as a binding partner of this domain. Nucleolin contains a long (~300 amino acids) intrinsically unstructured region, followed by the four tandem RNA recognition motifs and the C-terminal glycine/arginine-rich domain. Binding analyses revealed that NVL2^{UD} potentially binds to any of the combinations of two successive RNA binding domains in the presence of RNA. Furthermore, NVL2^{UD} has a characteristic loop, in which the key basic residues RRKR are exposed to the solvent at the edge of the molecule. The mutation study showed that these residues are necessary and sufficient for nucleolin-RNA complex binding as well as nucleolar localization. Based on the observations presented above, we propose that NVL2 serves as an unfoldase for the nucleolin-RNA complex. As inferred from its RNA dependence and its ATPase activity, NVL2 might facilitate the dissociation and recycling of nucleolin, thereby promoting efficient ribosome biogenesis.

Nuclear valosin-containing protein (VCP)[2]-like protein (NVL) was first identified as a gene product that displays a high level of amino acid similarity with an AAA-ATPase, VCP/p97. AAA-ATPases, associated with various cellular activities, are hexameric ATP-hydrolyzing enzymes found in all three kingdoms of life. They play important roles in various cellular processes, including the dissociation of protein complexes and protein translocation (1–4). The AAA-ATPases are characterized by the presence of one (type I) or two (type II) copies of a well conserved catalytic ATPase domain comprising 220–250 amino acids. NVL is classified as a type II AAA-ATPase with two tandem AAA domains. In fact, NVL has two alternatively spliced isoforms, a short form, NVL1, and a long form, NVL2, which are produced from different methionines as the translation initiation sites (Fig. 1) (5). NVL2 resides in the nucleolus, where it is involved in the biogenesis of the 60 S ribosomal subunit. In this pathway, the ribosomal subunit RPL5 and the DNA helicase DOB1 have been identified as NVL2-binding proteins (6, 7). Other well known NVL orthologs include *small-minded* (*smid*), a *Drosophila* ortholog (7, 8); a CED-4-interacting protein, Mac-1, a *Caenorhabditis elegans* ortholog (9); and a more distant *Saccharomyces cerevisiae* homolog, Rix7p (10, 11). The cellular roles of these nonvertebrate NVL orthologs are only partially consistent with each other. Consequently, further analysis of this molecule from a structural viewpoint is needed.

Despite the sequence similarity between VCP/p97 and NVL in their AAA regions, the N-terminal regions of NVL2 (NVL2^{UD}) and VCP/p97 are different. The two proteins reside in different subcellular locations; VCP/p97 is in the cytoplasm, nucleus, and endoplasmic reticulum membrane, whereas NVL is exclusively localized in the nucleolus (5, 6). The amino acid sequences of the N-terminal regions are variable, in contrast to the high sequence conservation of the AAA domains. The

---

[S] The on-line version of this article (available at http://www.jbc.org) contains supplemental Tables S1–S3 and Figs. S1–S4.

The atomic coordinates and structure factors (code 2rre) have been deposited in the Protein Data Bank, Research Collaboratory for Structural Bioinformatics, Rutgers University, New Brunswick, NJ (http://www.rcsb.org/).

The chemical shift assignments have been deposited in the BioMagResBank, under the accession code 11250 (http://www.bmrb.wisc.edu).

[1] To whom correspondence should be addressed. Tel.: 81-78-382-5813; Fax: 81-78-382-5816; E-mail: hiroakih@med.kobe-u.ac.jp.

---

[2] The abbreviations used are: VCP, valosin-containing protein; AAA, ATPases associated with various cellular activities; NVL, nuclear VCP-like protein; NVL2^{UD}, nuclear VCP-like protein 2 unique domain; NoLS, nucleolar localization signal; NTD, N-terminal domain; NSF, *N*-ethylmaleimide-sensitive fusion protein; NLS, nuclear localization signal; RRM, RNA recognition motif; GAR, glycine/arginine-rich; PDB, Protein Data Bank.

N-terminal regions of the AAA-ATPases are generally considered to contain a domain that is responsible for the specific role of the enzymes, such as adaptor binding, substrate specificity, or localization. The NVL2^{UD} has a nucleolar localization signal (NoLS) that is responsible for nucleolar targeting. Nagahama *et al.* (6) reported three separate regions as the nuclear and/or nucleolar localizing signals. Two of them exist in NVL2^{UD}. A stretch of basic amino acids, such as arginine and lysine, reportedly contributes to the nucleolar accumulation of proteins (12). Based on the nucleolar targeting sequences from several proteins, a simple motif, (R/K)(R/K)*X*(R/K), was proposed (13). The NoLS of NVL2 (residues 49–52) matches this classic definition.

The nucleolus comprises a high density complex of ribosomal DNA, ribosomal RNA, and its precursors, as well as many proteins. The primary physiological function of the nucleolus is ribosome biogenesis (14). However, recent studies revealed that the nucleolus plays other important roles in maintaining cellular viability, including RNA processing, specific mRNA stabilization, cell cycle control, and assembly of RNA viruses; for these reasons, it is implicated in cancer and other diseases (15–20). The nucleolus is organized and/or maintained using a network of protein-protein and protein-RNA/DNA interactions (21). Among the nucleolus interactome, two proteins, nucleolin and nucleophosmin, are considered as the key hub molecules. When each protein was knocked out or knocked down, the function as well as the structure of the nucleolus collapsed (22–24). Interactions with these hub proteins through the NoLS might direct the proteins to the nucleolus. Nevertheless, recently, the definition of the NoLS has become more complex, because many sequences that do not match the classic NoLS motif have been reported (reviewed in Ref. 21). The divergent NoLS sequences are considered to use a variety of pathways to target proteins to the nucleolus. It is proposed that the key action of the NoLS is to be recognized by one or more of the nucleolar resident proteins (21). Consequently, the mechanism-based classification of the NoLS has become important in this field.

The purpose of this study is to clarify the mechanism of the subcellular localization of NVL2 by a structural analysis of the N-terminal region of NVL2. Using a bioinformatics approach combined with a high throughput protein expression study, we isolated an "NMR-ready" domain (NVL2^{UD}, residues 1–74) from the N-terminal unique region of NVL2 (Fig. 1*A*) (25) and determined its three-dimensional structure using NMR. The solution NMR study revealed that the structure of NVL2^{UD} adopted part of the winged helix motif. The nucleolar localization signal is exposed on the molecular surface. We also confirmed that the domain solely exhibits the nucleolar localizing activity. Additionally, we identified the nucleolin C-terminal fragment as a binding target of NVL2^{UD} from HeLa cell extracts. The key residues responsible for nucleolar localization were identical to those for nucleolin binding. Finally, based on the "reversed" structural proteomics approach, we propose a physiological function for NVL2 in the nucleolus.

EXPERIMENTAL PROCEDURES

Reagents—DNA oligonucleotide primers were obtained from Hokkaido System Science Co. Ltd. (Sapporo, Japan). The anti-nucleolin antibodies were obtained from Santa Cruz Biotechnology, Inc. (Santa Cruz, CA) and Abcam (Cambridge, MA). Other chemicals were purchased from Wako Pure Chemical Industries Ltd. (Osaka, Japan) and Nacalai Tesque, Inc. (Kyoto, Japan).

Protein Techniques—The expression and purification of the N-terminal unique domains from mice were described previously (25). We used the GST fusion forms of NVL2^{UD} for biochemical assays. The proteins were expressed in *Escherichia coli* BL21(DE3), purified by chromatography on DEAE-Sepharose followed by glutathione-Sepharose affinity resin (GE Healthcare), and then dialyzed. We constructed plasmids for expressing GFP-tagged NVL2^{UD}(1–74) and NVL2^{UD}(1–74)AA in mammalian cells using the pcDNA-GFP-PRESAT vector, a pcDNA3.1-based vector containing the enhanced GFP gene with the PRESAT vector cloning site,[3] according to the modified protocol (26). We also constructed plasmids for expressing His$_6$-tagged human nucleolin fragments, R1234G (containing RRM domains 1–4 and the GAR domain (residues 286–710)), R123 (residues 286–560), R12 (residues 286–468), R23 (residues 391–560), R34 (residues 478–652), R34G (residues 478–710), R4G (residues 565–710), and R1 (residues 286–390), using the pET-His$_6$-PRESAT vector according to the reported method (27). The proteins were expressed in *E. coli* BL21(DE3).

NMR Structure Analysis—The preparation of isotopically labeled NMR samples of NVL2^{UD} was described previously (25). The NMR experiments and following structural determination are described in the supplemental material.

Cell Lines—We used HeLa and HEK293 cells in all experiments. The cells were cultured in Dulbecco's modified Eagle's medium (DMEM), supplemented with 10% (v/v) fetal bovine serum, 100 units/ml penicillin, and 100 units/ml streptomycin, and were incubated in humidified CO$_2$ containing (5%) air at 37 °C.

Mass Spectrometric Identification of the Proteins That Bind to NVL2^{UD}—Roughly 10^7 cells were collected, washed with PBS, and suspended in 200 μl of buffer containing 17.5 mM Tris-HCl (pH 7.5), 55 mM KCl, 1 mM MgCl$_2$, 1 mM EDTA, 0.5 mM EGTA, 1 mM DTT, 0.25 mM PMSF, 0.05% Triton X-100, and protease inhibitors (0.2 μg/ml antipain, 0.2 μg/ml aprotinin, 0.1 μg/ml leupeptin, 0.08 μg/ml pepstatin). After incubation on ice, the cells were disrupted by sonication. The whole cell extract was incubated with 180 pmol of either GST-NVL2^{UD}(1–93) or GST alone. Protein complexes were captured by glutathione-Sepharose. After washing three times, the resin was mixed with an equal volume of SDS loading dye. Protein complexes were resolved using SDS-PAGE and stained with Coomassie Brilliant Blue. In-gel proteolytic digestion followed by electrospray ionization tandem MS (LC-MS/MS) analysis was done at the Integrated Center for Mass Spectrometry (Graduate School of Medicine, Kobe University) using a mass spectrometer (*Q-TOF 2*; Micromass, Manchester, UK). Protein identification was performed using Mascot (Matrix Science).

Western Blotting Analysis—The HeLa cells were collected, washed with PBS, and suspended in 25 mM Tris-HCl (pH 7.5),

---

[3] N. Goda, T. Tenno, and H. Hiroaki, manuscript in preparation.

100 mM NaCl, 2 mM EDTA, 0.1% (v/v) Triton X-100, 1 mM DTT, 1 mM PMSF, and protease inhibitors. The cell extract was incubated with GST-NVL2^{UD}(1–74) or GST alone. Protein complexes were resolved by SDS-PAGE and blotted onto a PVDF membrane. We detected the nucleolin fragments using the anti-nucleolin antibody (catalog no. sc-17826, Santa Cruz Biotechnology, Inc.) followed by an HRP-conjugated anti-mouse IgG secondary antibody. The bands were visualized using a kit (ECL-Plus, GE Healthcare). An LAS-1000 detector (Fuji Film, Tokyo, Japan) was used for detection.

In Vitro Binding Assays—To assess the protein-protein interaction properties of NVL2^{UD} and nucleolin C-terminal fragments, a GST pull-down assay was conducted. GST or GST-NVL2^{UD} (140 pmol) was incubated with the *E. coli* cell lysate-expressed His$_6$-tagged nucleolin fragments in a buffer containing 25 mM Tris-HCl (pH 7.5), 120 mM KCl, 10% glycerol, 0.1% Triton X-100, 1 mM DTT, and protease inhibitors for 2 h at 4 °C and then immobilized on glutathione-Sepharose for 1 h. After three washes, an equal volume of SDS loading dye was added, and the proteins were fractionated by 12 or 15% SDS-PAGE. The gel was stained with Coomassie Brilliant Blue. The signal intensities were quantified by the ImageJ 1.40g program (National Institutes of Health, Bethesda, MD).

Fluorescent Microscopy—Cells were grown either on chamber slides (Matsunami Glass Ind. Ltd., Osaka, Japan), in normal 35-mm dishes, or on glass bottom 35-mm dishes (MatTek Corp.) to about 30% confluence. GFP-tagged-NVL2^{UD} or enhanced GFP alone was transfected using Lipofectamine 2000 (Invitrogen), according to the manufacturer's instructions. After 24 h of incubation, living cells were observed. For immunological staining, we washed the cells twice with PBS and fixed them with methanol for 20 min at −20 °C, washed them twice with PBS for 5 min, and then incubated them with the anti-nucleolin antibody in PBS supplemented with 5% skim milk overnight at 4 °C. The cells were then washed and incubated with a fluorescent secondary antibody (Cy3^{TM}-conjugated anti-mouse IgG antibody, C2181 (Sigma)) in PBS supplemented with 5% skim milk for 60 min. The cells were washed and then incubated with DAPI (final concentration, 100 ng/ml) in PBS at 5 min. The cells were then mounted in Prolong Antifade mounting medium (Invitrogen). All images were obtained using fluorescence microscopy with a microscope equipped with a color CCD camera system (IX71 and DP-70, respectively; Olympus, Tokyo, Japan).

RESULTS

Structural Analysis of Mouse NVL2^{UD}—The final ensemble of the 20 lowest energy structures of NVL2^{UD}(1–74) was generated from a total of 994 experimental constraints derived by NMR. A representative image is presented in Fig. 2*B*. Supplemental Table S1 and supplemental Fig. S1 show that the resulting structures satisfy the experimental constraints well. The stereochemical quality of the ensemble is good, with >91% of the backbone ϕ-ψ angles occupying the most favored or allowed regions in the Ramachandran plot (supplemental Table S1 and supplemental Fig. S1). Excluding the disordered regions that are the N- and C-terminal residues and parts of internal loops (residues 1–10 plus the extra four residues from the vec-

tor, residues 28, 49–51, and 71–74), the root mean square deviation values are 0.418 Å for the backbone heavy atoms and 1.035 Å for all heavy atoms. Based on the refined structure of NVL2^{UD}, we conducted a multiple sequence alignment of the domains among the NVL orthologs, using a secondary structure-based penalty (Fig. 1*B*). Although the amino acid identities among these NVL homologs are not high (19–86%), the residues forming the hydrophobic core as well as the second loop connecting helices 2 and 3 are well conserved. Consequently, the N-terminal regions of the NVL2 homologs are novel structural domains with similar folds.

NVL2^{UD}(1–74) adopts an orthogonal three-helix fold, which consists of helix 1 (residues 11–23), helix 2 (residues 32–42), and helix 3 (residues 52–70) (Fig. 2*A*). A structural comparison of NVL2^{UD}, using the DaliLite server (28), identified many proteins containing a winged helix domain with Z-scores higher than 4.5. For example, the structures of the DNA binding domain of a transcription factor, DP2 (PDB code 1cf7, Z-score 5.2), and the Zα domain of a double-stranded RNA deaminase I, ADAR1 (PDB code 1qgp, Z-score 4.5) and that of the 34L protein (PDB code 1sfu, Z-score 4.5) resembled the NVL2^{UD} structure. In addition, the partial structures of cullin-1 (PDB code 1ldj, Z-score 4.8), FurB (PDB code 2o03, Z-score 4.7), replication terminator protein (PDB code 1f4k, Z-score 4.7), and NEDD8 (PDB code 3dqv, Z-score 4.6) were retrieved. The presence of this fold was not predicted by several structure prediction methods, including FUGUE (29) and FORTE (30). As described below, NVL2^{UD} contains the NoLS. This motif resides in the second loop region, which is exposed to the solvent.

Identification of the Nucleolin C-terminal Fragment as the Binding Target of NVL2^{UD}—To identify new NVL2^{UD}-associated proteins, we performed an *in vitro* protein-binding experiment followed by an electrospray ionization-MS/MS analysis. We used HeLa whole cell extracts to identify the partner proteins associated with NVL2^{UD}(1–93). The Coomassie Brilliant Blue staining of the affinity-captured proteins revealed several polypeptides that specifically co-purified with GST-NVL2^{UD} (Fig. 3*A*). In comparison with the proteins associated with GST alone, we carefully examined a specifically enriched protein band at 30 kDa. The MS analysis revealed that most NVL2^{UD}-binding proteins were related to RNA processing or the nucleolus (Table 1 and supplemental Table S2). It is particularly interesting that some potential NVL2^{UD}-binding proteins harbor RRM domains, although none of these binding proteins has previously been reported to interact with NVL2. As shown in Table 1, nucleolin is the second candidate of the NVL2^{UD}-binding partners. Nucleolin is an abundant protein in the nucleolus and is the putative NoLS receptor. Therefore, we further addressed this link between nucleolin and NVL2. A question remained as to the difference between the theoretical molecular mass of full-length nucleolin (M_r 76,614) and that of the analyzed band (30 kDa). We confirmed the existence of full-length nucleolin in both the NVL2^{UD}(1–74) and NVL2^{UD}(1–93)-associated proteins, using a Western blot analysis (Fig. 3*B* and supplemental Fig. S2). We detected full-length nucleolin by two distinct antibodies, sc-17826 (epitope: 271–520) and ab22758 (epitope: 1–100). The full-length nucleolin showed a band at 95 kDa, probably because of phosphorylation. We detected several
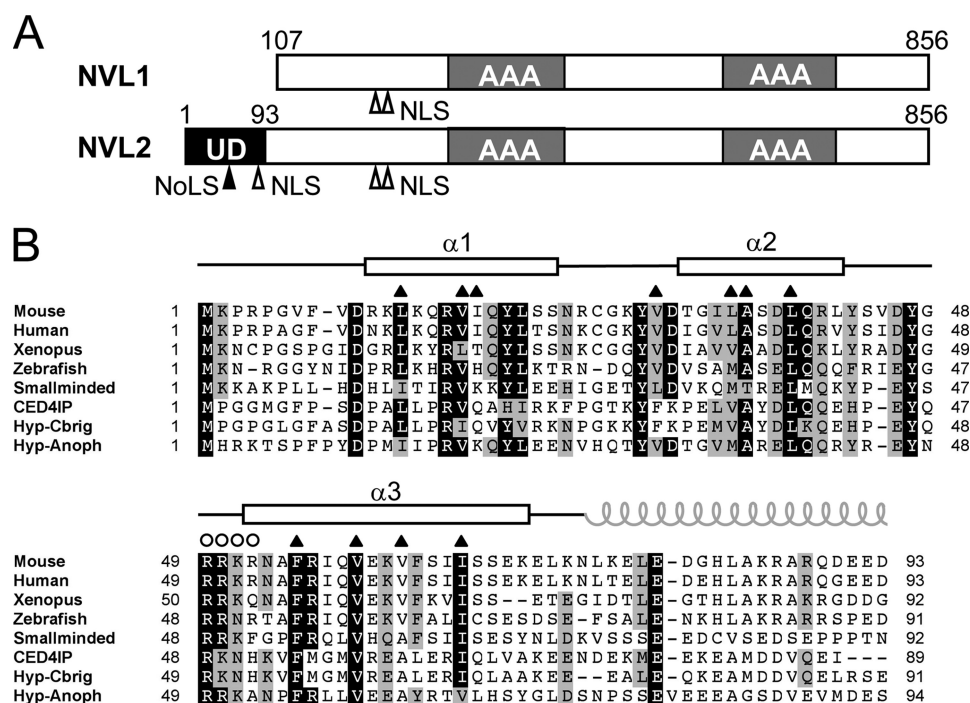
FIGURE 1. **Domain architecture of NVL and multiple sequence alignment of the NVL2^{UD}.** *A*, domain arrangement of NVL1 and NVL2. Two splicing variants of human NVL are shown. The translation of NVL1 starts at the second methionine of NVL2. The unique domain is isolated from the N-terminal region specific for NVL2. The *filled arrowhead* and *open arrowheads* indicate NoLS and NLS, respectively. *UD*, NVL2 unique domain; *AAA*, AAA domain. *B*, multiple sequence alignment of NVL2 orthologs. The secondary structure elements of NVL2^{UD}(1–74) are shown at the *top* of the diagram with *open boxes* (α-helix). The residues in the hydrophobic core and the NoLS are indicated by *triangles* and *circles*, respectively. The *gray spiral* represents the coiled-coil region. Protein names and UniProtKB accession numbers are as follows: mouse (Q9DBY8), human (O15381), *Xenopus* (Q7ZXI4), zebrafish (P91638), *smallminded* (P91638), CED4IP (*C. elegans*; Q9U8KO), Hyp-Cbrig (*Caenorhabditis briggsae*; A8XYN0), and Hyp-anoph (*Anopheles*; Q7Q5U3). The sequence alignment was generated using ClustalX (70).
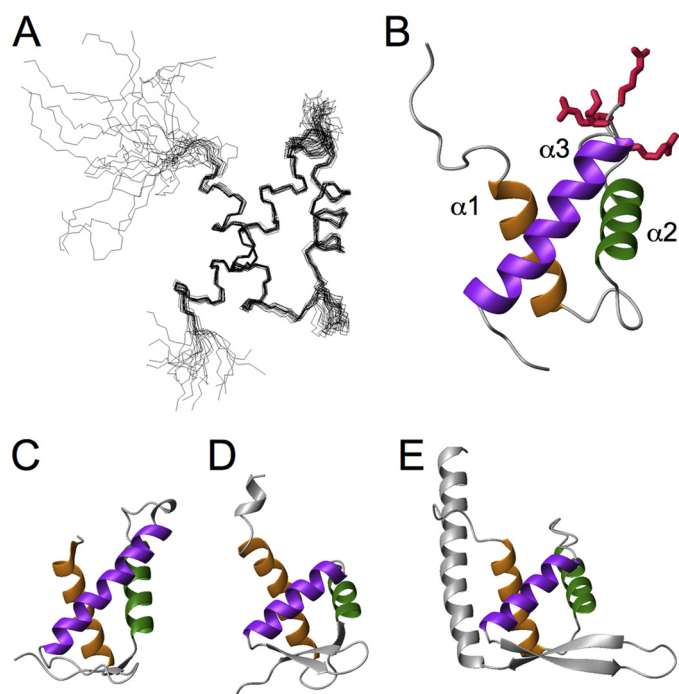

FIGURE 2. **Structure of NVL2^{UD}.** *A*, a superposition of the backbone atoms of the 20 lowest energy structures. *B*, *ribbon diagram* of NVL2^{UD}, with the NoLS residues shown as *sticks*. *C–E*, the structural neighbors of NVL2^{UD}. The Dali server was used to identify proteins structurally similar to NVL2^{UD}. The corresponding helices are *colored* the same (helices 1, 2, and 3 are *orange*, *green*, and *dark violet*, respectively). *C*, DP2 (PDB code 1cf7). *D*, ADAR1 (PDB code 1qgp). *E*, replication terminator protein (PDB code 1f4k). All *panels* were prepared using MOLMOL (71).

shorter nucleolin fragments with the sc-17826 antibody. The shorter fragments are attributed to the degradation of its unstructured N-terminal region during sample preparation. The N-terminal region contains proteolytic sites (31). The association of nucleolin with NVL2^{UD}(1–74) and NVL2^{UD}(1–93) was also detected using HEK293 cells, although the full-length nucleolin in the cell extract was more rapidly degraded than that in the HeLa cell extract, despite the use of increased amounts of the protease inhibitors (supplemental Fig. S2).

NVL2^{UD} Potentially Binds to Two or More Successive RNA Binding Domains of Nucleolin—Human nucleolin contains 710 amino acids. It is divided roughly into three regions: N-terminal, central, and C-terminal domains. The N-terminal domain is rich in acidic residues and is predicted as natively disordered. The central domain contains four repeats of RRM domains. The C-terminal GAR domain is rich in glycine and arginine. Both the RRM and GAR domains are RNA binding domains (32). Because the peptide sequence detected by the MS/MS analysis corresponded to the C terminus of the fourth RRM domain (Fig. 3*C*), we prepared the recombinant nucleolin, R1234G (residues 286–710, containing the four RRM and the C-terminal GAR domains), and examined its interaction with NVL2^{UD}. The R1234G interacted with NVL2^{UD} specifically, thus suggesting that this region of nucleolin was sufficient for NVL2^{UD} binding (Fig. 4, *A* and *B*).

To define the minimum region responsible for NVL2^{UD} binding by nucleolin, we expressed several fragments of nucleolin in *E. coli* and examined their NVL2^{UD} binding ability.
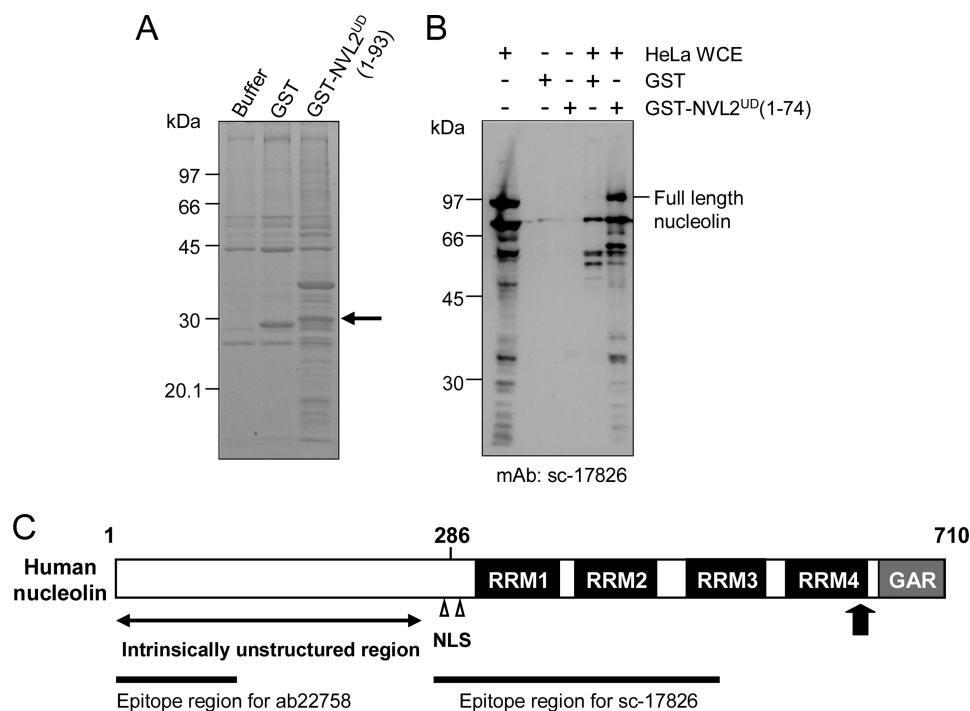
FIGURE 3. **NVL2^{UD} is a nucleolin binding domain.** *A*, *in vitro* binding assay of GST-NVL2^{UD} with a HeLa cell extract. GST-NVL2^{UD}(1–93)-associated proteins were separated by SDS-PAGE and stained with Coomassie Brilliant Blue. The band indicated by an *arrow* was subjected to the MS/MS analysis. *B*, Western blot of HeLa proteins captured by GST-NVL2^{UD}. GST or GST-NVL2^{UD}(1–74) was incubated with either HeLa whole cell extract (*WCE*) or buffer, and co-purified proteins were electrophoresed. The proteins were blotted onto a PVDF membrane and then detected by an anti-nucleolin antibody. The epitope for the antibody is residues 271–520 of human nucleolin. *C*, domain architecture of human nucleolin. The *arrow* marks the position of the peptide sequence detected by the MS/MS analysis. The RRM domains and the GAR domain are shown as *black* and *gray boxes*, respectively, with the domain names.

TABLE 1

List of protein candidates identified from mass spectrometric analysis

Protein	Molecular mass	Score[a]
	kDa	
Ribosomal protein L7	29.7	113
Nucleolin	76.6	86
Leucine-rich repeat-containing 59	34.5	83
Heterogeneous nuclear ribonucleoprotein C	33.6	80
Progesterone receptor membrane component 2	23.8	78
Proteasome subunit α type 5	26.4	75
Heterogeneous nuclear ribonucleoprotein D	30.4	70
Heterogeneous nuclear ribonucleoprotein A	37.0	68
Proteasome subunit α type 7	27.9	63
Prohibitin	23.6	62
Vimentin	20.0	62

[a] Score determined as $-10 \log(P)$, where P is the probability that the observed match is a random event, calculated by the program MASCOT. A score >54 indicates extensive homology, $p < 0.05$.

Almost all of the fragments (R123, R34G, R12, R23, R34, and R4G) except for R1 retained affinity for NVL2^{UD} (Fig. 4, *B* and *C*). In detail, R123 and R34G showed higher affinity than the others, and R34 showed the lowest affinity. Because the sequence identity among the four RRMs is not high (20–38%), it is unlikely that NVL2^{UD} recognizes a certain common motif or surface among the four RRM domains (supplemental Fig. S3). We propose another mechanism, in which two or more successive RNA binding domains (RRM and GAR) are responsible for NVL2^{UD} binding with promiscuous recognition. Additionally, we expected that the interaction between NVL2^{UD} and nucleolin is not accomplished by simple protein-protein binding. We examined whether the purified R12 interacted with NVL2^{UD}, using NMR titration experiments with R12 and ^{15}N-labeled NVL2^{UD} (supplemental Fig. S4). No significant chemical shift perturbations were observed, suggesting the involvement of additional factors for their interaction.

RNA Enhances the Interaction between NVL2^{UD} and Nucleolin—According to the unusual observation described above, we examined the effect of RNA on the nucleolin-NVL interaction. The nucleolus contains highly condensed RNAs, especially preribosomal RNA, and thus RNA could affect the interaction between NVL2^{UD} and nucleolin. To test this possibility, we added RNase A to the pull-down assay, and the specific interaction disappeared (Fig. 4*D*). This result revealed that RNA is necessary for the NVL2-nucleolin interaction. Therefore, NVL2^{UD} might bind to the nucleolin-RNA complex in which more than two successive RNA binding domains hold the RNA.

The RRKR Motif in NVL2^{UD} Is Necessary and Sufficient for Nucleolar Targeting—In fact, NVL2^{UD} contains the classic NoLS consensus, (R/K)(R/K)X(R/K), at residues 49–52. When the RRKR motif was substituted to RRAA, the nucleolar accumulation of NVL2 was lost (6). To examine whether these residues contribute to the RNA-mediated NVL2-nucleolin interaction, we used the NVL2^{UD} RRAA mutant (NVL2^{UD}AA) (Fig. 4*D*). The NVL2^{UD}AA could not interact with nucleolin, irrespective of the presence of RNA. Next, to examine the relationship between the nucleolin-NVL2^{UD} interaction and the nucleolar localization of NVL2^{UD}, we compared the cellular localizations of NVL2^{UD} and NVL2^{UD}AA. Whereas NVL2^{UD} accumulated in the nucleus and mainly in nucleoli, almost all of the NVL2^{UD}AA remained in the cytoplasm and did not localize to the nucleolus (Fig. 5). These results demonstrated that
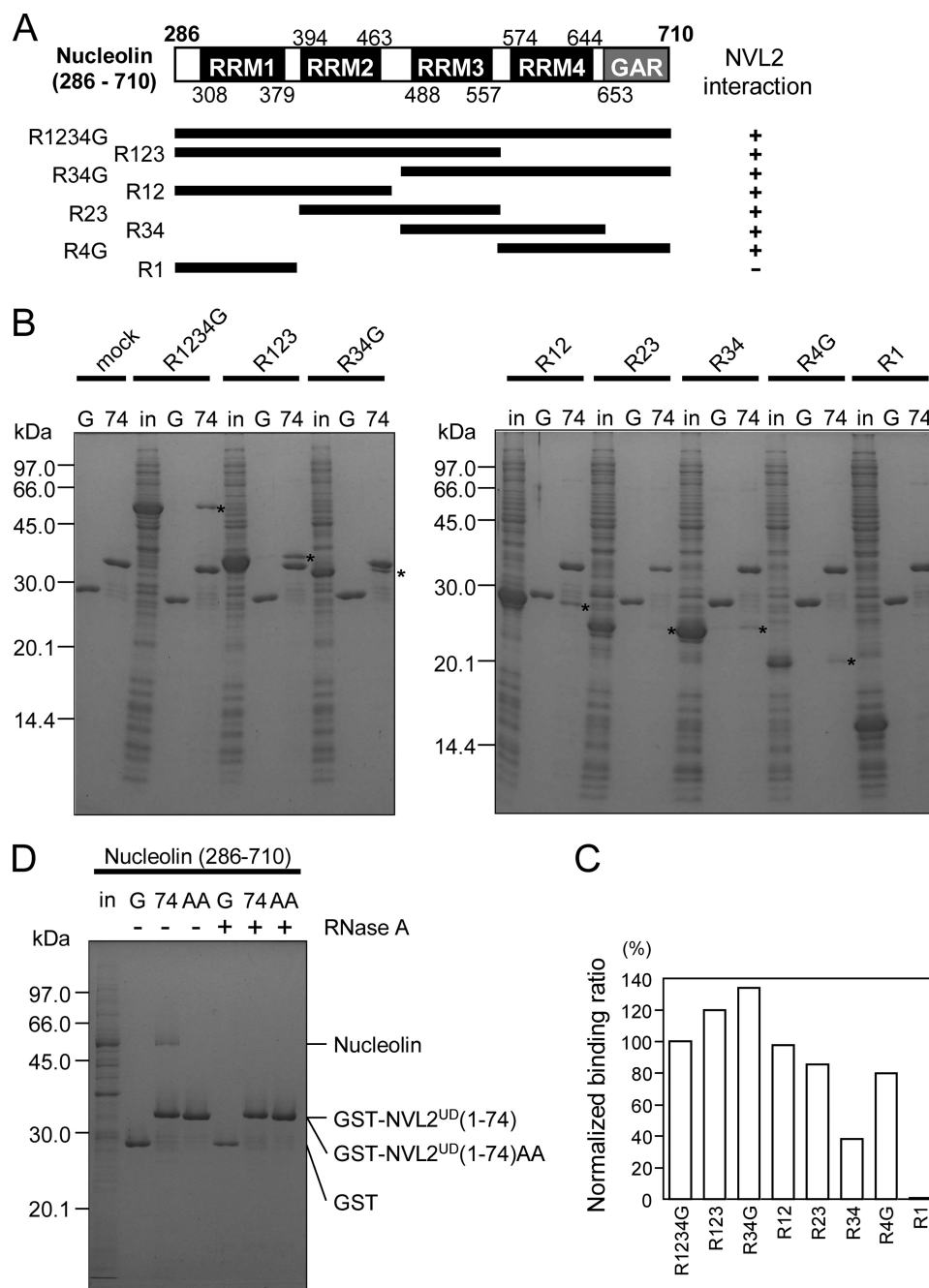
FIGURE 4. **Interaction between NVL2^{UD} and nucleolin.** *A*, summary of the binding assays between NVL2^{UD} and various nucleolin fragments. *B*, *in vitro* binding assay with nucleolin fragments. Either GST (*G*) or GST-NVL2^{UD}(1–74) (*74*) was incubated with *E. coli* cell lysates expressing various nucleolin fragments (*in*). The bound proteins were pulled down and separated using 15% SDS-PAGE. The gel was stained with Coomassie Brilliant Blue. *Asterisks* denote the nucleolin fragments bound to NVL2^{UD}(1–74). *C*, quantification of the nucleolin fragments bound to GST-NVL2^{UD}(1–74). The signals corresponding to the nucleolin fragments in *B* were integrated and normalized by their molecular weights, using ImageJ. *D*, RNA is involved in the NVL2-nucleolin complex. An *in vitro* binding assay was conducted with nucleolin (R1234G) and wild-type or mutant NVL2^{UD}(1–74) in the presence or absence of RNase A.

NVL2^{UD} is an isolated domain sufficient for the nucleolar localization of NVL2 and that the nucleolar localization of NVL2^{UD} requires its interaction with the nucleolin-RNA complex.

DISCUSSION

Nucleolar Localization Motif within NVL2^{UD}—We identified NVL2^{UD}, a small globular domain, which contains a "classic" nucleolar localization signal consensus sequence, (R/K)(R/K)X(R/K), in its structured region. Recent studies have shown

that the classic description of nucleolar localization signals must be changed and expanded drastically. This results from the complex pathway of the nucleolar localization of proteins, in contrast to the nuclear localization signal (NLS), which encodes the recognition sequence of the dominant NLS receptors, importins. To date, no common NoLS signal recognition molecule has been identified, unlike the importins and exportins for NLS and nuclear export signal. Instead, many proteins involved in the nucleolar protein-protein interaction network is
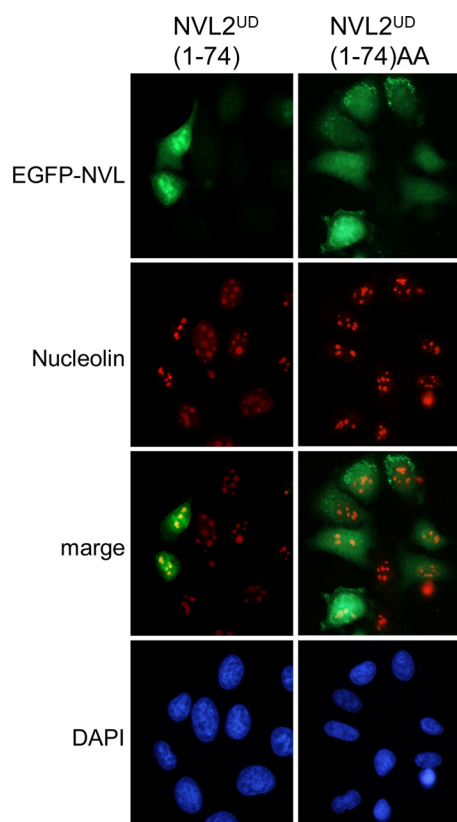
FIGURE 5. **NVL2[UD] is a nucleolus localization domain.** HeLa cells were transfected with GFP-NVL2[UD](1–74) or GFP-NVL2[UD](1–74)AA. After a 24-h incubation, cells were fixed, stained with anti-nucleolin antibody and DAPI, and then visualized.

FIGURE 6. **Comparison of NoLS structures with the NVL2[UD].** Shown are NoLS-containing structures selected from the list of Emmott and Hiscox (21). The electrostatic surface representations are superimposed on the *ribbon diagrams*. Positive (*blue*) and negative (*red*) electrostatic potentials of each molecule are mapped on the van der Waals surfaces. NoLSs are depicted as *sticks* and are *colored red* (Arg and Lys) or *orange* (all residues except Arg and Lys). *A*, NVL2[UD] (PDB code 2rre); *B*, MDM2 ring finger domain (PDB code 2hdp); *C*, HIV-1 Tat (PDB code 1k5k); *D*, HIV-1 Rev (PDB code 2x7l); *E*, IBV-N protein (PDB code 2bxx).

responsible for nucleolar localization (21). Our results revealed that the RRKR motif in NVL2[UD] plays a role in both nucleolar targeting and retention. The association with the nucleolin-RNA complex might contribute to the nucleolar retention of NVL2. This supports the network model for nucleolar localization.

From this viewpoint, we tried to identify a structural consensus of the NoLS, by comparing the structure and the surface properties of NVL2[UD] with other known NoLS-containing structures. We chose the representative NoLSs from the recent nucleolar targeting review by Emmott and Hiscox (21). Among them, we found six unique structures in the Protein Data Bank with the following PDB codes: 1k5k (HIV-1 Tat), 1etf (HIV-1 Rev peptide-RNA), 2bxx (IBV-N protein), 2hdp (MDM2), 2fgf (FGF2), and 2ang (angiogenin). These proteins, except for FGF2 and angiogenin, interact with many of the major nucleolar components: nucleolin, nucleophosmin, and RNA. HIV-1 Tat and HIV-1 Rev interact with either nucleophosmin or RNA directly through the NoLS, and the solution structure of the HIV-1 Rev peptide-RNA complex was solved (33–37). Nucleophosmin also plays an important role in its interaction with MDM2 (38). Regarding MDM2, its C-terminal ring finger domain, containing the NoLS as well as the N-terminal region, is responsible for nucleophosmin binding. On the other hand, RNA binds to the extended RNA binding site containing the NoLS of IBV-N protein (39). Among them, MDM2 and IBV-N protein reportedly interact with nucleolin (40, 41). A positively charged cluster covers most of the surfaces of these molecules
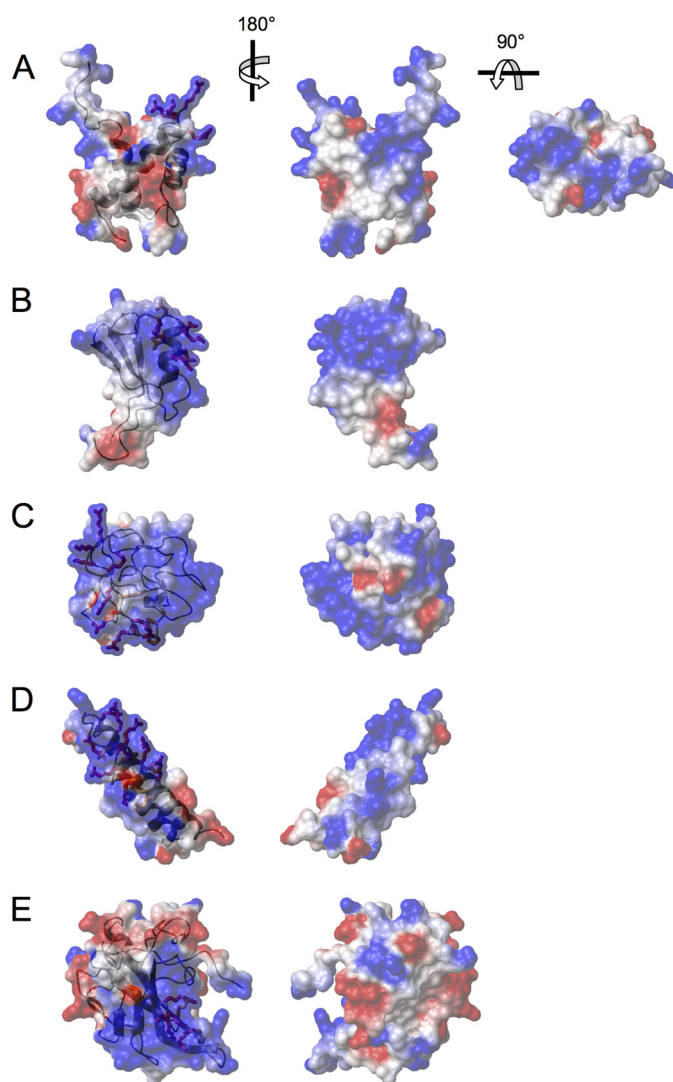
(Fig. 6), suggesting that charge-charge interactions are important for nucleolar localization. Moreover, most of the arginines and lysines in the NoLS, the key residues for nucleolar localization, are exposed on the edge of the molecule. The NoLS of NVL2[UD] forms a positively charged protrusion at the top edge of the domain; however, the charge distribution is unique, in that the positively charged clusters are separately positioned. Interestingly, HIV-1 Tat and Rev have exposed side chains with RNA recognizing arginines and lysines, which are suitable for base interactions with structured RNA. The NoLS of NVL2[UD] adopts a similar exposed conformation, thereby suggesting the affinity for RNA. Although the direct contribution of the NoLSs to their nucleolin binding was not examined for MDM2 and IBV-N protein, the NoLS of MDM2 forms the prominent protrusion at the top of the convex surface of the positive cluster. We presume that MDM2 interacts with nucleolin in a manner

FIGURE 7. **Summary of the type II AAA-ATPases.** Domain architecture, subcellular localization, target proteins, and functions of type II AAA-ATPases are indicated. Each AAA-ATPase dissociates the target from the protein complex. Because the removed proteins are used again in the following assembly cycle for the respective complex, we propose that the recycling of target proteins is a function of the type II AAA-ATPases.

similar to NVL2[UD]. To our knowledge, NVL2[UD] is the first domain found to be responsible for nucleolar localization through an interaction with the nucleolin RRM domains.

Molecular Architecture of NVL Compared with Other Type II AAA-ATPases; Classification with Type II AAA-ATPases—Fig. 7 presents a summary of the similarities and the differences of the type II AAA-ATPases, with their domain architectures. For the conserved NTDs of the other type II AAA-ATPases, extensive structural-functional studies of NSF (42–47), VCP (p97) (48–55), and PEX1 have been reported (56–58). NSF and its yeast ortholog, Sec18, are responsible for heterotypic membrane fusion mainly in exocytic pathways (46–48). The α-, β-, and γ-soluble NSF attachment proteins are the most important targets of NSF (42). VCP and yeast CDC48 are involved in endoplasmic reticulum-associated protein degradation (49–51) as well as in remodeling of the Golgi and nuclear membrane (48, 52). Although the specific targets of the VCP and CDC48 unfoldase activities remain unclear, they have various cellular functions involving many different adaptor and anchor molecules, such as p37 (59), p47 (52), Ufd1/Npl4 (51), VCIP135 (53), Derlin-1, and VIMP (54). These different VCP adaptors might control VCP functions. Actually, PEX1 has a slightly different domain architecture, with the common NTD, followed by a unique insertion of ~300 residues, and the AAA domains (D1 and D2). Although the NTD of PEX6 has not been determined, the FORTE structure prediction server revealed a high Z-score for the homologue to PEX1[NTD].[4]

This figure clearly shows that NVL (and its orthologs) are structurally distinct from the other type II AAA-ATPases. For example, NVL only works at the nucleolus and not on the surface of the membranous organelle. The smaller NTD (NVL2[UD]) and insertion lengths between the domains are characteristic. Moreover, NVL2[UD] can be eliminated by alternative splicing. Nevertheless, some common features with these type II AAA-ATPases are still visible. In general, all of these enzymes form a

hexameric ring and can act as protein unfoldases. Most of the type II AAA-ATPases are located in organelle membranes, where they are involved in specific functions, such as membrane fusion (42, 43, 48) and protein transport across the membrane (49, 60–62). The process of protein-protein and/or protein-membrane association is self-driving and thereby ATP-independent. In contrast, the reversal processes, in which protein-protein/protein-lipid interactions are dissociated, often require ATP energy generated by AAA-ATPases. These reversal processes are necessary for the next cycle of the complex formation for many biological events, such as membrane fusion and peroxisomal protein transport. Consequently, the common feature of the known type II AAA-ATPases is to reuse and/or to recycle the molecular machinery.

Role of NVL in the Nucleolus—In contrast to the other membrane-related AAA-ATPases, we found that NVL2[UD] functions through a nucleolin-RNA complex at nucleoli. Nucleolin is a hub protein of the network of multiple protein-protein interactions in the nucleolus, which preserves the nucleolus structure. Nucleolin harbors a long, natively disordered region with a cluster of acidic amino acids, which might serve as a scaffold for many nucleolin-binding proteins (21). Recent studies have shown that intrinsically unstructured proteins and regions play key roles in protein-protein interaction networks, especially in the hub proteins in many interactomes (63, 64). Nevertheless, the results of the present study showed that NVL2[UD] binds to the RNA binding regions of nucleolin in an RNA-dependent manner but not to the intrinsically unstructured region. This feature distinguishes the role of NVL2 from those of the other nucleolin-binding proteins, such as topoisomerase I and histone H1. As mentioned above, the conserved NTDs of the other type II AAA-ATPases, except for NVL, are involved in binding to either adaptor proteins or substrates. Similarly, nucleolin may be the NVL2 adaptor that NVL2 works with or one of the NVL2 substrates.

If nucleolin is the NVL2 adaptor, then the ATP-hydrolyzing energy of NVL2 is transferred to nucleolin. It then promotes

---

[4] H. Hiroaki, K. Tomii, N. Goda, and H. Watabe, unpublished result.

dissociation of the protein-protein interaction between the disordered region and the nucleolin partner proteins. Although the nucleolar resident proteins drastically alter their members, according to the cell cycle and extracellular stimuli (17), the mechanism of this dynamic nucleolar remodeling has remained unclear. Therefore, we propose NVL2 as one candidate for the master molecule of nucleolar functions. On the other hand, the latter case, in which nucleolin is the direct substrate of the NVL2 ATPase activity and NVL2 promotes nucleolin dissociation from its target RNAs, is also likely.

Our results suggest that NVL2^{UD} can act on any pair of successive RRM domains in the presence of RNA rather than on one particular RRM domain. In other words, the RRMs and the following GAR domain seem to act redundantly for NVL2^{UD} binding, as presumed by the different molecular surfaces of the four RRMs. For example, the conserved surface residues of the RRMs are no greater than 20%, as deduced by comparing their solution structures (PDB codes 2rkk, 2fc9, and 2fc8, respectively) (65).[5] Moreover, the locations of the identical residues differ among them. This surface variation results in the different specificity to RNA. For example, the first and second RRM domain pairs are tightly bound to the specific stem-loop RNA (rGGCCGAAAUCCCGAAGUAGGCC) in the complex structure (66). This RNA merely interacts with the third and fourth RRM domains (67). Nevertheless, these four RRMs were functionally redundant *in vivo*, especially for RNA processing during ribosome biogenesis, although the efficiency of the RNA processing was different (68). Taken together, we concluded that NVL2^{UD} recognizes the nucleolin-RNA complex in a promiscuous manner, which is not dependent on either a specific protein-protein interaction or a specific RNA sequence. It is more likely that the target of NVL2^{UD} is a certain structural element, such as a looped out RNA between two successive RNA binding domains of nucleolin. This idea arises from the mechanism of the HIV-Tat-RNA interaction, in which the peptide also acts as a nucleolar localization signal sequence for HIV-Tat. In that case, two arginine residues in the basic peptide promote tight binding of Tat to the RNA stem loop, with an interaction termed the "arginine fork" (69). We hypothesize that the mechanism of nucleolin interaction by NVL2^{UD} resembles that of HIV-Tat, in which the side chains of the RRKR motif grasp the RNA loops formed by nucleolin RNA binding domains. We showed that the RNA mixture of unknown sequences, which is eventually contaminated from *E. coli* extract, enhanced the NVL2^{UD}-nucleolin interaction. Additional work is necessary to clarify the molecular basis of NVL2^{UD} recognition of the nucleolin-RNA complex.

Proteins containing RRM domains reportedly interact with their specific RNA sequences. It is assumed that nucleolin binds to its unique binding motifs, which are included in preribosomal RNA. The affinity between nucleolin and the target RNA is increased by the simultaneous interaction of successive RNA binding domains. Therefore, the existence of an active mechanism to release nucleolin from RNAs is favorable. Indeed, this theory is supported by the observation that the dominant neg-
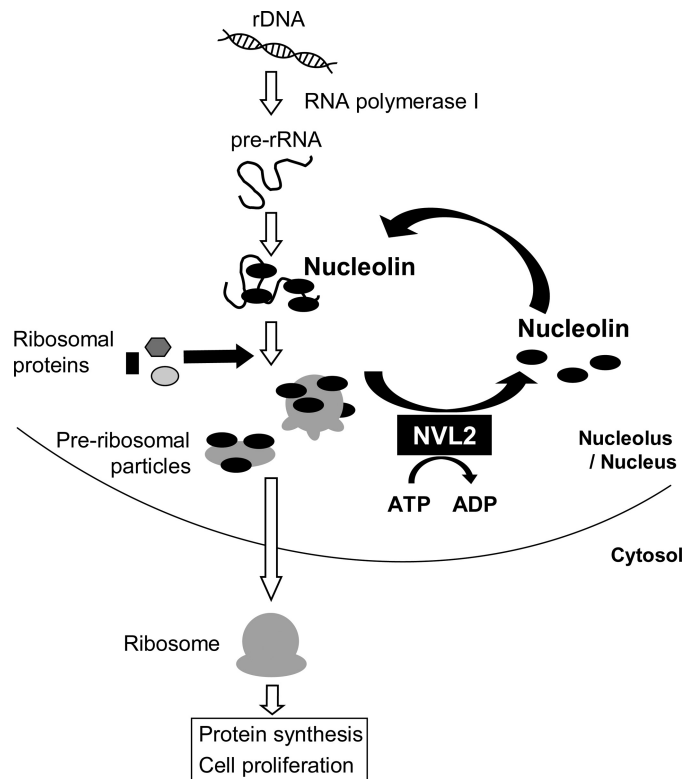

FIGURE 8. **Model for the function of NVL2 in ribosome biogenesis.** In ribosome biogenesis, nucleolin plays a role in rDNA transcription and maturation. Nucleolin binds to rRNA via its RRM domains, and it may regulate ribosome maturation. NVL might dissociate the nucleolin RRM domains from the rRNA with energy derived from ATP hydrolysis to promote some steps, such as protein incorporation or rRNA folding. The released nucleolin interacts with other rRNA molecules as well as rDNA. Consequently, NVL recycles nucleolin at the nucleolus.

ative NVL2 mutant suppresses 60 S ribosomal subunit biogenesis (6). A possible mechanism of ribosome biogenesis control by NVL2 is shown in Fig. 8.

In conclusion, we solved the structure of the N-terminal unique domain of NVL2. We identified nucleolin as a new target for NVL2. Our results showed that RNA enhances the interaction between NVL2^{UD} and nucleolin, in which the NoLS of NVL2 played the key role for their interaction. In fact, NVL2^{UD} recognized any two or more successive RNA binding domains of nucleolin. By analogy to the other type II AAA-ATPases, we propose that NVL dissociates the nucleolin-RNA complex to promote ribosome biogenesis.

REFERENCES

1. Lupas, A. N., and Martin, J. (2002) *Curr. Opin. Struct. Biol.* **12,** 746–753
2. Patel, S., and Latterich, M. (1998) *Trends Cell Biol.* **8,** 65–71
3. Neuwald, A. F., Aravind, L., Spouge, J. L., and Koonin, E. V. (1999) *Genome Res.* **9,** 27–43
4. Ogura, T., and Wilkinson, A. J. (2001) *Genes Cells* **6,** 575–597
5. Germain-Lee, E. L., Obie, C., and Valle, D. (1997) *Genomics* **44,** 22–34

[5] S. Yokoyama, unpublished result.

6. Nagahama, M., Hara, Y., Seki, A., Yamazoe, T., Kawate, Y., Shinohara, T., Hatsuzawa, K., Tani, K., and Tagaya, M. (2004) *Mol. Biol. Cell* **15,** 5712–5723

7. Long, A. R., Yang, M., Kaiser, K., and Shepherd, D. (1998) *Gene* **208,** 191–199

8. Long, A. R., Wilkins, J. C., and Shepherd, D. (1998) *Mech. Dev.* **76,** 33–43

9. Wu, D., Chen, P. J., Chen, S., Hu, Y., Nuñez, G., and Ellis, R. E. (1999) *Development* **126,** 2021–2031

10. Kressler, D., Roser, D., Pertschy, B., and Hurt, E. (2008) *J. Cell Biol.* **181,** 935–944

11. Gadal, O., Strauss, D., Braspenning, J., Hoepfner, D., Petfalski, E., Philippsen, P., Tollervey, D., and Hurt, E. (2001) *EMBO J.* **20,** 3695–3704

12. Siomi, H., Shida, H., Nam, S. H., Nosaka, T., Maki, M., and Hatanaka, M. (1988) *Cell* **55,** 197–209

13. Weber, J. D., Kuo, M. L., Bothner, B., DiGiammarino, E. L., Kriwacki, R. W., Roussel, M. F., and Sherr, C. J. (2000) *Mol. Cell. Biol.* **20,** 2517–2528

14. Cmarko, D., Smigova, J., Minichova, L., and Popov, A. (2008) *Histol. Histopathol.* **23,** 1291–1298

15. Montanaro, L., Treré, D., and Derenzini, M. (2008) *Am. J. Pathol.* **173,** 301–310

16. Greco, A. (2009) *Rev. Med. Virol.* **19,** 201–214

17. Hernandez-Verdun, D. (2006) *Histochem. Cell Biol.* **126,** 135–148

18. Matthews, D. A., and Olson, M. O. (2006) *EMBO Rep.* **7,** 870–873

19. David, M. J., Martindill, D. M., and Riley, P. R. (2008) *Cell Cycle* **7,** 17–23

20. Stark, L. A., and Taliansky, M. (2009) *EMBO Rep.* **10,** 35–40

21. Emmott, E., and Hiscox, J. A. (2009) *EMBO Rep.* **10,** 231–238

22. Ugrinova, I., Monier, K., Ivaldi, C., Thiry, M., Storck, S., Mongelard, F., and Bouvet, P. (2007) *BMC Mol. Biol.* **8,** 66

23. Ma, N., Matsunaga, S., Takata, H., Ono-Maniwa, R., Uchiyama, S., and Fukui, K. (2007) *J. Cell Sci.* **120,** 2091–2105

24. Amin, M. A., Matsunaga, S., Uchiyama, S., and Fukui, K. (2008) *Biochem. J.* **415,** 345–351

25. Iwaya, N., Goda, N., Unzai, S., Fujiwara, K., Tanaka, T., Tomii, K., Tochio, H., Shirakawa, M., and Hiroaki, H. (2007) *J. Biomol. NMR* **37,** 53–63

26. Goda, N., Tenno, T., Takasu, H., Hiroaki, H., and Shirakawa, M. (2004) *Protein Sci.* **13,** 652–658

27. Tenno, T., Goda, N., Tateishi, Y., Tochio, H., Mishima, M., Hayashi, H., Shirakawa, M., and Hiroaki, H. (2004) *Protein Eng. Des. Sel.* **17,** 305–314

28. Holm, L., and Rosenström, P. (2010) *Nucleic Acids Res.* **38,** W545–W549

29. Shi, J., Blundell, T. L., and Mizuguchi, K. (2001) *J. Mol. Biol.* **310,** 243–257

30. Tomii, K., and Akiyama, Y. (2004) *Bioinformatics* **20,** 594–595

31. Pasternack, M. S., Bleier, K. J., and McInerney, T. N. (1991) *J. Biol. Chem.* **266,** 14703–14708

32. Ghisolfi, L., Kharrat, A., Joseph, G., Amalric, F., and Erard, M. (1992) *Eur. J. Biochem.* **209,** 541–548

33. Weeks, K. M., Ampe, C., Schultz, S. C., Steitz, T. A., and Crothers, D. M. (1990) *Science* **249,** 1281–1285

34. Li, Y. P. (1997) *J. Virol.* **71,** 4098–4102

35. Tan, R., Chen, L., Buettner, J. A., Hudson, D., and Frankel, A. D. (1993) *Cell* **73,** 1031–1040

36. Szebeni, A., Herrera, J. E., and Olson, M. O. (1995) *Biochemistry* **34,** 8037–8042

37. Battiste, J. L., Mao, H., Rao, N. S., Tan, R., Muhandiram, D. R., Kay, L. E., Frankel, A. D., and Williamson, J. R. (1996) *Science* **273,** 1547–1551

38. Kurki, S., Peltonen, K., Latonen, L., Kiviharju, T. M., Ojala, P. M., Meek, D., and Laiho, M. (2004) *Cancer Cell* **5,** 465–475

39. Tan, Y. W., Fang, S., Fan, H., Lescar, J., and Liu, D. X. (2006) *Nucleic Acids Res.* **34,** 4816–4825

40. Saxena, A., Rorie, C. J., Dimitrova, D., Daniely, Y., and Borowiec, J. A. (2006) *Oncogene* **25,** 7274–7288

41. Chen, H., Wurm, T., Britton, P., Brooks, G., and Hiscox, J. A. (2002) *J. Virol.* **76,** 5233–5250

42. Clary, D. O., Griff, I. C., and Rothman, J. E. (1990) *Cell* **61,** 709–721

43. Dalal, S., Rosser, M. F., Cyr, D. M., and Hanson, P. I. (2004) *Mol. Biol. Cell* **15,** 637–648

44. Yu, R. C., Jahn, R., and Brunger, A. T. (1999) *Mol. Cell* **4,** 97–107

45. Lenzen, C. U., Steinmann, D., Whiteheart, S. W., and Weis, W. I. (1998) *Cell* **94,** 525–536

46. Whiteheart, S. W., and Kubalek, E. W. (1995) *Trends Cell Biol.* **5,** 64–68

47. Hay, J. C., and Scheller, R. H. (1997) *Curr. Opin. Cell Biol.* **9,** 505–512

48. Rabouille, C., Levine, T. P., Peters, J. M., and Warren, G. (1995) *Cell* **82,** 905–914

49. Rabinovich, E., Kerem, A., Fröhlich, K. U., Diamant, N., and Bar-Nun, S. (2002) *Mol. Cell. Biol.* **22,** 626–634

50. Ye, Y., Meyer, H. H., and Rapoport, T. A. (2003) *J. Cell Biol.* **162,** 71–84

51. Meyer, H. H., Shorter, J. G., Seemann, J., Pappin, D., and Warren, G. (2000) *EMBO J.* **19,** 2181–2192

52. Kondo, H., Rabouille, C., Newman, R., Levine, T. P., Pappin, D., Freemont, P., and Warren, G. (1997) *Nature* **388,** 75–78

53. Uchiyama, K., Jokitalo, E., Kano, F., Murata, M., Zhang, X., Canas, B., Newman, R., Rabouille, C., Pappin, D., Freemont, P., and Kondo, H. (2002) *J. Cell Biol.* **159,** 855–866

54. Ye, Y., Shibata, Y., Kikkert, M., van Voorden, S., Wiertz, E., and Rapoport, T. A. (2005) *Proc. Natl. Acad. Sci. U.S.A.* **102,** 14132–14138

55. Zhang, X., Shaw, A., Bates, P. A., Newman, R. H., Gowen, B., Orlova, E., Gorman, M. A., Kondo, H., Dokurno, P., Lally, J., Leonard, G., Meyer, H., van Heel, M., and Freemont, P. S. (2000) *Mol. Cell* **6,** 1473–1484

56. Weller, S., Gould, S. J., and Valle, D. (2003) *Annu. Rev. Genomics Hum. Genet.* **4,** 165–211

57. Shiozawa, K., Maita, N., Tomii, K., Seto, A., Goda, N., Akiyama, Y., Shimizu, T., Shirakawa, M., and Hiroaki, H. (2004) *J. Biol. Chem.* **279,** 50060–50068

58. Shiozawa, K., Goda, N., Shimizu, T., Mizuguchi, K., Kondo, N., Shimozawa, N., Shirakawa, M., and Hiroaki, H. (2006) *FEBS J.* **273,** 4959–4971

59. Uchiyama, K., Totsukawa, G., Puhka, M., Kaneko, Y., Jokitalo, E., Dreveny, I., Beuron, F., Zhang, X., Freemont, P., and Kondo, H. (2006) *Dev. Cell* **11,** 803–816

60. Tamura, S., Shimozawa, N., Suzuki, Y., Tsukamoto, T., Osumi, T., and Fujiki, Y. (1998) *Biochem. Biophys. Res. Commun.* **245,** 883–886

61. Fujiki, Y., Okumoto, K., Otera, H., and Tamura, S. (2000) *Cell Biochem. Biophys.* **32,** 155–164

62. Fujiki, Y., Miyata, N., Matsumoto, N., and Tamura, S. (2008) *Biochem. Soc. Trans.* **36,** 109–113

63. Higurashi, M., Ishida, T., and Kinoshita, K. (2008) *Protein Sci.* **17,** 72–78

64. Hegyi, H., Schad, E., and Tompa, P. (2007) *BMC Struct. Biol.* **7,** 65

65. Arumugam, S., Miller, M. C., Maliekal, J., Bates, P. J., Trent, J. O., and Lane, A. N. (2010) *J. Biomol. NMR* **47,** 79–83

66. Allain, F. H., Bouvet, P., Dieckmann, T., and Feigon, J. (2000) *EMBO J.* **19,** 6870–6881

67. Serin, G., Joseph, G., Ghisolfi, L., Bauzan, M., Erard, M., Amalric, F., and Bouvet, P. (1997) *J. Biol. Chem.* **272,** 13109–13116

68. Storck, S., Thiry, M., and Bouvet, P. (2009) *Biol. Cell* **101,** 153–167

69. Tao, J., and Frankel, A. D. (1992) *Proc. Natl. Acad. Sci. U.S.A.* **89,** 2723–2726

70. Thompson, J. D., Gibson, T. J., Plewniak, F., Jeanmougin, F., and Higgins, D. G. (1997) *Nucleic Acids Res.* **25,** 4876–4882

71. Koradi, R., Billeter, M., and Wüthrich, K. (1996) *J. Mol. Graph.* **14,** 51–55